Spectrochimica Acta Part A: Molecular and Biomolecular Spectroscopy 103 (2013) 222–231

Contents lists available at SciVerse ScienceDirect

Spectrochimica Acta Part A: Molecular and Biomolecular Spectroscopy

journal homepage: www.elsevier.com/locate/saa

Molecular structure and spectroscopic analysis of 1,4-Bis(1-methyl-2-benzimidazolyl)benzene; XRD, FT-IR, dispersive-Raman, NMR and DFT studies

Bilge Eren [a,*], Arslan Ünal [b]

[a] Department of Chemistry, Science and Arts Faculty Bilecik Şeyh Edebali University, 11210 Bilecik, Turkey
[b] Department of Physics, Science and Arts Faculty Bilecik Şeyh Edebali University, 11210 Bilecik, Turkey

HIGHLIGHTS

- 1,4-Bis(1-methyl-2-benzimidazolyl)benzene was synthesized under microwave conditions.
- It was characterized by using XRD, FT-IR, dispersive-Raman, NMR and DFT.
- Conformational analysis was also carried out.
- A complete assignments of the vibrational modes were proposed.
- The theoretical results were compared with the experimental findings.

GRAPHICAL ABSTRACT

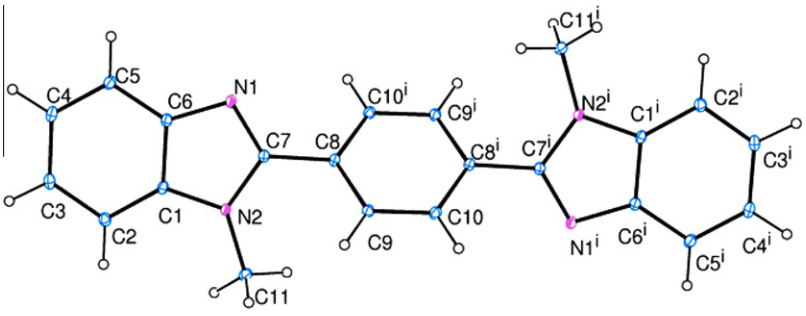

ARTICLE INFO

Article history:
Received 9 August 2012
Received in revised form 5 October 2012
Accepted 10 October 2012
Available online 7 November 2012

Keywords:
1,4-Bis(1-methyl-2-benzimidazolyl)benzene
Bis-benzimidazole
XRD
Vibrational spectra
NMR
DFT

ABSTRACT

This study reports the structural characterization of a bis-benzimidazole derivative, 1,4-Bis(1-methyl-2-benzimidazolyl)benzene (BMBB), by using spectroscopic and quantum chemical methods. The BMBB molecule was synthesized under microwave conditions and was characterized by using single-crystal X-ray diffraction, FT-IR, dispersive Raman and NMR spectroscopies. The potential energy surface scan study was carried out for the conformation of the theoretical structure. Quantum chemical calculations of relative energies, molecular geometry, vibrational wavenumbers, frontier molecular orbitals, atomic charges and gauge including atomic orbital (GIAO) ^{1}H and ^{13}C-NMR chemical shifts of the compound were carried out by using density functional method (DFT) at B3LYP/6-311++G(d,p) theory level. The complete assignments of the vibrational modes were performed with DFT calculations combined with scaled quantum mechanics force field (SQMFF) methodology. A satisfactory consistency between the experimental and theoretical findings was obtained. On account of the relative energies, population analysis and XRD results, the most stable conformational form of the molecule was also determined.

Introduction

Vibrational (IR, Raman) and NMR spectroscopies are extensively used in order to investigate dynamical and structural properties of molecules. With the recent developments in computational methods, it is possible to describe molecular properties of molecules with close chemical accuracy using theoretical methods [1,2]. The density functional theory (DFT) calculations using B3LYP method shows good agreement with the experimental data at molecular electrostatic potentials, bond energies, optical properties, vibrational frequencies and geometric parameters of organic compounds [3–11].

Bis-benzimidazoles are an important class of bioactive molecules in the field of chemistry and pharmacology. Bis-benzimidazole

* Corresponding author. Tel.: +90 228 214 1481; fax: +90 228 216 0080.
E-mail address: bilge.eren@bilecik.edu.tr (B. Eren).

1386-1425/$ - see front matter © 2012 Elsevier B.V. All rights reserved.
http://dx.doi.org/10.1016/j.saa.2012.10.055

derivatives have been found to possess varied *pharmacological* activities such as antimicrobial [12–14], antifungal [15], and anti-tumoral [16–18] effects. In addition, bis-benzimidazole derivatives are used in industrial processes as membranes for direct methanol fuel cells [19] or in dye-sensitized solar cells [20]. The wide ranges of applications on bis-benzimidazole compounds have attracted many scientists to investigate the structural and spectral behaviors of bis-benzimidazoles that necessary for understanding their chemical or biological properties.

In our previous work, we have reported the synthesis and structural characterization of some 2-substituted benzimidazoles by using experimental and theoretical methods [8,9]. To the best of our knowledge, no evidence of similar studies on bis(2-benzimidazoles) have been reported in the open chemical literature to date. In continuation of our work, herein, 1,4-Bis(1-methyl-2-benzimidazolyl)benzene (BMBB) was synthesized under neat microwave conditions. The BMBB compound was characterized by using single-crystal X-ray diffraction, FT-IR, dispersive-Raman, ^{13}C and ^{1}H NMR spectroscopies. In addition, a detailed conformational analysis by DFT/B3LYP/6-311++G(d,p) theory level was performed and the theoretical data of stable four conformers were compared with experimental spectroscopic findings. A complete assignment of the vibrational modes was performed with the help of the potential energy distributions (PEDs) values by using the scaled quantum force field (SQMFF) methodology. In addition, frontier molecular orbitals (FMOs), and natural bond orbitals (NBOs) analysis were performed at the same level of theory. These calculations are also valuable for providing insight into molecular parameters, vibrational and NMR spectra. The aim of this work is to explore the structural parameters and spectroscopic features of the title compound that rule its chemical behavior.

Experimental

Instrumentation

All the chemicals and solvents were of the highest analytical grade and used as supplied. Reactions under microwave irradiation were performed in a modified domestic microwave oven (Bosch HMT 812C). Reactions were monitored by thin-layer chromatography (TLC) on silica–gel 60 F254 plates (Merck) and an UV lamp. The melting point was determined using a capillary tube and a digital melting point apparatus (Gallenkamp Electrothermal) and was uncorrected. The ATR–IR spectrum of BMBB was recorded in the range of (4000–500 cm^{-1}) region with a Bruker Vertex 80v FTIR spectrometer. The FT-IR (4000–400 cm^{-1}) spectra between KBr windows as Nujol or 1,3-hexachlorobutadiene mulls of the sample were recorded via a Bruker Optics IFS66v/s FTIR spectrometer with 2 cm^{-1} resolution in vacuum. The dispersive Raman spectrum was recorded using a Bruker Senterra Dispersive Raman microscope spectrometer at 532 nm excitation from a doubled Nd/YAG laser having 3 cm^{-1} resolution between 4000 and 60 cm^{-1} spectral region. The ^{1}H and ^{13}C-NMR spectra were recorded on a Bruker Avence II-400 MHz NMR spectrometer using tetramethylsilane (TMS) as an internal standard and DMSO-d_6 as solvent. Crystallographic data were recorded on a Bruker Kappa APEXII CCD area detector diffractometer using Mo Kα radiation (k = 0.71073 Å) at T = 100 K.

Synthesis of 1,4-Bis(1-methyl-2-benzimidazolyl)benzene

The 1,4-Bis(1-methyl-2-benzimidazolyl)benzene ($C_{22}H_{18}N_4$) compound was obtained by condensation of N-methyl-o-phenylenediamine with the $NaHSO_3$ adduct of terephthalaldehyde according to Ridley et al. [21], but under neat microwave conditions; Terephthalaldehyde 2.73 g (20 mmol) was dissolved in 40 ml ethanol and $NaHSO_3$ 4.16 g (40 mmol) in 20 ml water was added in portions. The mixture was stirred vigorously an hour in an ice bath. The precipitate was $NaHSO_3$ adduct of terephthalaldehyde, filtered as white solid and dried under vacuo 6.65 g (yield: 97%). 2 mmol (0.24 g, 0.234 ml) N-methyl-o-phenylenediamine and 1.2 mmol (0.41 g) $NaHSO_3$ adduct of terephthalaldehyde were mixed. After adding a few drops of dimethylformamide, the mixture was irradiated in a modified domestic microwave oven for 35 min until the reaction was completed according to the TLC data. The mixture was cooled and poured into ice cold water under vigorous stirring. The precipitate was collected by filtration, washed with water and dried (0.27 g, yield: 80%, m.p. 281–283 °C. The suitable single crystals for X-ray analysis were obtained by recrystallisation from ethanol/water. The synthesis procedure of 1,4-Bis(1-methyl-2-benzimidazolyl)benzene is shown in Scheme 1.

X-ray crystallography

A suitable colorless block-shaped crystal sample of size 0.18 mm × 0.26 mm × 0.45 mm was chosen for the crystallographic study. All diffraction measurements were performed at 100 K using graphite monochromated Mo Kα radiation (k = 0.71073 Å) in ω-scanning mode. Details of the data collection conditions and parameters of refinement process are given in Table 1.

Calculations

Potential energy surfaces (PESs) of 1,4-Bis(1-methyl-2-benzimidazolyl)benzene molecule were primarily obtained in order to get the most stable conformer. Therefore, PES were determined via MOPAC2002 geometry optimization by using semi-empirical PM5 Hamiltonian within Fujitsu CAChe WS Pro v.7.5.0 Windows software package [22] on a personal workstation for the possible stable structures of BMBB, where the torsion angles τ_1(N1C7C8C10^i), τ_2(N2^{i}C7^{i}C8^{i}C9^i), τ_3(C1N2C11H11A) and τ_3(C1^{i}N2^{i}C11^{i}H11A^i) were changed by 3°. The appropriate structures were then selected by considering the heat of formation energy (ΔH) values were lower than 132.00 kcal/mol.

For the selected structures, local minima or transition states on the PES were then examined through geometric optimization and vibrational frequency analysis by using Becke's three-parameter exchange functional [3] in combination with the Lee–Yang–Parr correlation functional [23] (B3LYP) method with 6-311++G(d,p) basis set by using the Gaussian 03W program package [24]. The result of complete geometry optimization and vibrational frequency analysis computations indicate that BMBB has only four stable conformers which are adopted C_1 point group containing no symmetry element. Before calculating vibrational and NMR properties of the conformers, the other appropriate point groups such as C_i, C_2, and C_s were taken into account and the stability of each conformers were also tested at the same level of theory.

The PED corresponding to each of the observed vibrational wavenumbers were calculated by using SQMFF which show the relative contributions of the redundant internal coordinates to each vibrational mode of the molecule and thus make it possible to describe the character of each mode numerically [25,26]. The relative Raman intensity (I^R), which simulates the measured Raman spectrum, was calculated by using the following relation derived from the intensity theory of Raman scattering [7];

$$I_i^R = \frac{f(v_0 - v_i)^4 S_i}{v_i[1 - \exp(-hcv_i/kT)]} \quad (1)$$

where v_0 is the exciting frequency (18,798 cm^{-1}), v_i is the vibrational wavenumber of the ith normal mode (in cm^{-1} units), S_i is

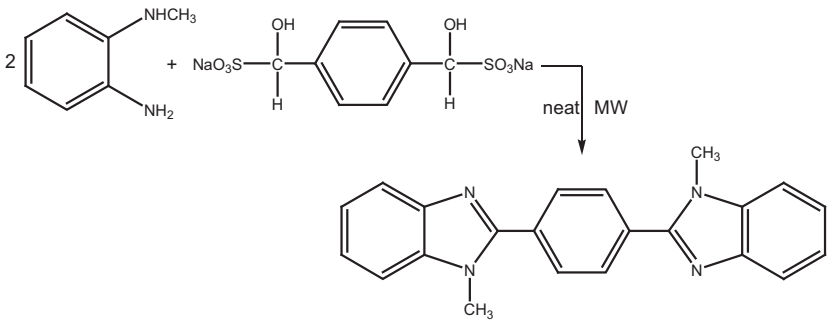

Scheme 1. Synthesis of 1,4-Bis(1-methyl-2-benzimidazolyl)benzene.

the Raman scattering activity of the normal mode q_i, h, c, and k are fundamental constants, $T = 298.15$°K and $f(2 \times 10^{-15})$ is a suitably chosen common normalization factor for all peaks. For the plots of simulated IR and Raman spectra, pure Lorentzian band shapes were used with a bandwidth of 10 cm^{-1}.

Main atomic charges of non-hydrogen atoms using the natural population analysis (NPA) analysis and frontier molecular orbitals were obtained at the same level of theory. For the NMR calculations, the stable four conformers of BMBB were initially reoptimized at B3LYP/6-311++G(d,p) theory level in DMSO-d_6 using the by using the integral equation formalism polarizable continuum model (IEFPCM) method [27,28]. After optimization, ^{1}H and ^{13}C NMR isotropic shielding tensors of BMBB were calculated GIAO method [29,30] in DMSO-d_6 at the same theory level as implemented in Gaussian 03W program package. Isotropic shielding tensors of ^{13}C and ^{1}H were changed into chemical shifts by using a linear relationship suggested by Alyar et al. [10].

Results and discussion

Stability of the conformers

The results of the computations have clearly demonstrated that 1,4-Bis(1-methyl-2-benzimidazolyl)benzene molecule has four possible stable conformers at room-temperature. The calculated relative energies of these possible stable conformers at B3LYP/6-311++G(d,p) theory level is presented in Table 2 with respect to the zero point energy (ZPE), self-consistent field (SCF) and Gibbs free energy (ΔG). On account of the relative energies, population analysis and XRD results, Conformer1 was found to be the most stable conformer and was only considered in the crystallographic and vibrational spectral analysis.

Geometrical structure

The optimized geometric structure of Conformer1 and the obtained XRD structure of 1,4-Bis(1-methyl-2-benzimidazolyl)benzene are shown in Fig. 1. The experimental and optimized geometrical parameters (bond lengths, bond and dihedral angles) of BMBB obtained at B3LYP/6-311++G(d,p) are listed in Table 3.

According to obtained experimental XRD results, BMBB crystallizes in the monoclinic space group *P 21/c* with two molecules in the unit cell. The BMBB molecule is composed of two 1-methylbenzo[d]imidazole groups and a benzene ring. The benzene and benzimidazole rings of the molecule are not coplanar and have a dihedral angle of 43.48 (7)°. Furthermore, the dihedral angle between the five- and six-membered rings of the benzimidazole ring system is 1.80 (7)°. The crossed torsion angles at the junction, N1—C6—C1—C2 and C5—C6—C1—N2, are found −177.87(11)° and 179.01(10)°. The steric effect of the methyl substitution at N2 atom

Table 1
Crystal data and structure refinement parameters for 1,4-Bis(1-methyl-2-benzimidazolyl)benzene.

CCDC deposition no.	886,035
Color/shape	Colorless/block
Chemical formula	C22 H18 N4
Formula weight	338.40
Temperature (K)	100
Wavelength (Å)	0.71073 Mo Kα
Crystal system	Monoclinic
Space group	*P 21/c*
Symmetry space group name Hall	−P 2ybc
Unit cell parameters	
a, *b*, *c* (Å)	17.7652(7), 4.3867(2), 10.9717(4)
Volume (Å^3)	816.77(6)
Z	2
Calculated density (Mg/m^3)	1.376
μ (mm^{-1})	0.084
T_{min}, T_{max}	0.974, 0.985
F_{000}	356.00
Crystal size (mm^3)	0.18 × 0.26 × 0.45
Structure solution	Direct methods
Corrections applied	Lorentz-polarization
Index ranges	$-23 \leqslant h \leqslant 23$, $-5 \leqslant k \leqslant 5$, $-14 \leqslant l \leqslant 14$
Theta range for data collection (°)	$1.20 \leqslant \theta \leqslant 28.61$
Measured reflections	1842
Independent/observed reflections	13328/2079
R_{int}	0.0422
Refinement method	Full-matrix least-squares on F^2
Data/restraints/parameters	13328/0/397
Goodness-of-fit on F^2	1.120
R indices [$I > 2\sigma(I)$]	$R_1 = 0.0422$, w$R_2 = 0.1119$
R indices (all data)	$R_1 = 0.0482$, w$R_2 = 0.1255$
$\Delta\rho_{max}$, $\Delta\rho_{min}$ (e/Å^3)	0.385, −0.301

Table 2
The selected molecular properties of the possible stable conformers of BMBB at DFT B3LYP method with 6-311++G(d,p) basis set.

	Conformer1[a]	Conformer2	Conformer3	Conformer4
Symmetry	C_i	C_2	C_2	C_s
μ_{TOTAL} (Debye)	0.00	4.29	4.84	6.64
ΔSCF (kcal/mol)	0.00	0.33	0.48	0.88
ΔG (kcal/mol)	0.00	0.45	0.49	0.67
N_i (%)	44.89	21.00	19.63	14.48
Torsion angle (°)				
τN1C7C8C10^i	−36.20	−33.74	−38.12	−34.37
τN2C7C8C10^i	144.17	146.44	142.18	146.00
τN1^{i}C7^{i}C8^{i}C10	36.20	−33.74	139.41	−142.32
τN2^{i}C7^{i}C8^{i}C10	−144.17	146.44	−40.28	37.34
τC1N2C11H11A	154.37	152.50	155.14	153.17
τC1^{i}N2^{i}C11^{i}H11A^i	−154.37	152.50	155.14	−153.17
τN1C7C7^{i}N1^i	180.00	108.79	−78.23	0.03
τN1C7C7^{i}N2^i	−0.52	−70.46	101.38	179.94

[a] The relative energies of the conformers were given in respect to the calculated self-consistent field (SCF), zero point energy (ZPE) and Gibbs free energy (ΔG) of Conformer1. The SCF and ΔG energies of Conformer1 are −670488.31 kcal/mol and −670299.12 kcal/mol.

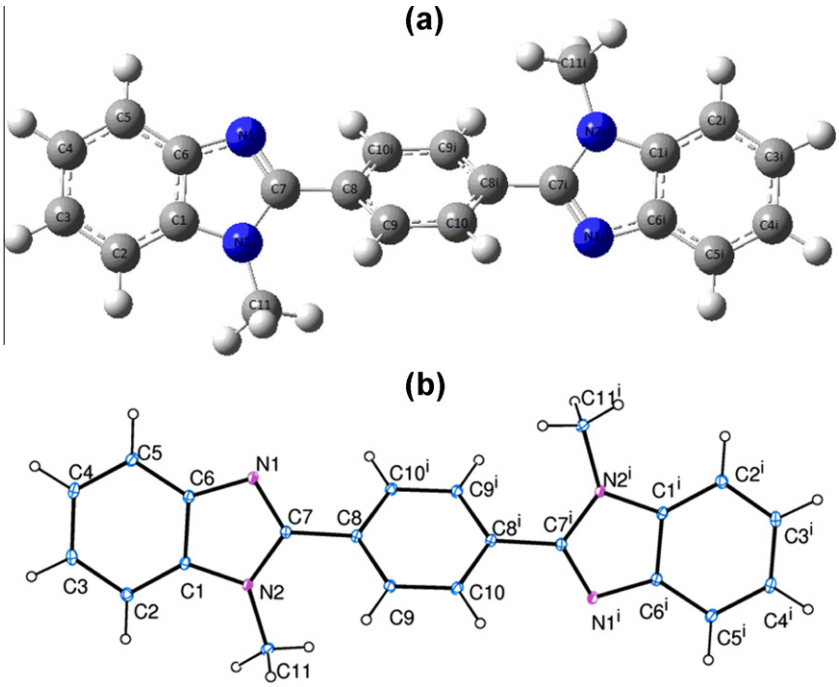

Fig. 1. The molecular structure of 1,4-Bis(1-methyl-2-benzimidazolyl)benzene: (a) Conformer1, calculated; (b) XRD, experimental.

Table 3
The experimental geometrical parameters of BMBB compound and comparison with calculated data of the Conformer1 at B3LYP/6-311++G(d,p) theory level.

Parameters[a]	X-ray	Conformer1	Difference	Parameters[a]	X-ray	Conformer1	Difference
Bond lengths (Å)				*Bond angles (°)*			
C1—C2	1.3940(16)	1.3956	−0.0016	N2—C7—C8	124.06(10)	124.39	−0.33
C2—C3	1.3855(16)	1.3912	−0.0057	C7—N1—C6	104.32(10)	105.70	−1.38
C3—C4	1.4010(18)	1.4082	−0.0072	C7—N2—C1	106.26(9)	106.18	0.08
C4—C5	1.3817(17)	1.3889	−0.0072	C11—N2—C1	125.08(10)	124.13	0.95
C5—C6	1.3976(15)	1.3995	−0.0019	C11—N2—C7	128.35(9)	129.14	−0.79
C6—C1	1.4023(16)	1.4127	−0.0104	*Torsion angles (°)*			
C7—C8	1.4700(15)	1.4705	−0.0005	C3—C4—C5—C6	0.30(19)	0.05	0.25
C8—C9	1.4010(15)	1.4032	−0.0022	C4—C3—C2—C1	−0.15(18)	−0.01	−0.14
C8—C10i	1.3943(16)	1.4018	−0.0075	C5—C4—C3—C2	0.15(19)	0.13	0.02
C9—C10	1.3849(15)	1.3884	−0.0035	C6—C1—C2—C3	−0.31(17)	−0.32	0.01
N1—C6	1.3887(14)	1.3796	0.0091	C7—C8—C9—C10	−179.49(11)	−177.98	−1.51
N1—C7	1.3201(15)	1.3164	0.0037	C8—C9—C10—$C8^i$	0.30(2)	0.44	−0.14
N2—C1	1.3801(13)	1.3848	−0.0047	C10—C8—C9—$C10^i$	−0.30(2)	−0.43	0.13
N2—C7	1.3723(15)	1.3907	−0.0184	C4—C5—C6—N1	177.59(12)	177.64	−0.05
N2—C11	1.4545(15)	1.4554	−0.0009	C7—N1—C6—C5	−178.53(12)	−179.76	1.23
Bond angles (°)				C7—N1—C6—C1	−0.08(13)	−0.25	0.17
C1—C2—C3	116.39(11)	116.81	−0.42	C1—N2—C7—C8	−179.11(10)	−179.16	0.05
C2—C3—C4	121.61(11)	121.50	0.11	C5—C6—C1—N2	179.01(10)	179.95	−0.94
C3—C4—C5	121.52(11)	121.39	0.13	C7—N2—C1—C6	−0.50(12)	−0.31	−0.19
C4—C5—C6	118.01(11)	118.01	−0.00	C7—N2—C1—C2	177.52(12)	179.67	−2.15
C5—C6—C1	119.63(11)	119.93	−0.30	N2—C1—C2—C3	−178.04(11)	−179.60	1.56
C6—C1—C2	122.83(10)	122.37	0.46	C6—N1—C7—N2	−0.26(13)	−0.46	0.20
C7—C8—C9	121.69(10)	121.92	−0.23	N1—C6—C1—N2	0.37(13)	0.04	0.33
C7—C8—$C10^i$	119.27(10)	118.62	0.65	C1—N2—C7—N1	0.50(13)	0.50	0.00
C8—C9—C10	120.27(11)	120.83	−0.56	C11—N2—C1—C2	3.50(2)	7.49	−3.99
C9—C8—C10i	119.03(10)	118.41	0.62	C11—N2—C1—C6	−174.52(10)	−171.88	−2.64
C9—C10—$C8^i$	120.69(10)	120.75	−0.06	C11—N2—C7—C8	−5.36(18)	−9.18	3.82
N1—C6—C1	110.29(10)	109.97	0.32	C11—N2—C7—N1	174.26(11)	171.16	3.10
N1—C6—C5	130.06(11)	130.06	0.00	N1—C6—C1—C2	−177.87(11)	−179.49	1.62
N1—C7—C8	122.32(10)	122.93	−0.61	N1—C7—C8—C9	136.40(12)	141.35	−4.95
N1—C7—N2	113.62(10)	112.68	0.94	N2—C7—C8—C9	−44.03(17)	−38.28	−5.75
N2—C1—C2	131.62(11)	132.16	−0.54	N1—C7—C8—$C10^i$	−42.82(17)	−36.20	−6.62
N2—C1—C6	105.52(10)	105.47	0.05	N2—C7—C8—$C10^i$	136.75(12)	144.17	−7.42

[a] Coordinate descriptions are carried out by the numbers as in Fig. 1.

Table 4
Intermolecular interactions of 1,4-Bis(1-methyl-2-benzimidazolyl)benzene.

D—H···A	D—H (Å)	H···A (Å)	D···A (Å)	D—H···A (°)
C11—H11B···Cg1[a]	0.98	2.89	3.408(14)	114
C11—H11B···N2[a]	0.98	3.00	3.601(16)	121
C11—H11C···N1[b]	0.98	2.86	3.784(16)	158
C9—H9···N1[b]	0.95	3.06	3.993(15)	168
C5—H5···N2[c]	0.95	3.09	3.934(15)	148

Cg1: The centroid of the C6—C7 ring.
[a] *x*, *y* + 1, *z*.
[b] *x*, 1/2−*y*, *z* + 1/2.
[c] *x*, 1/2−*y*, 1/2−*z*.

Table 5
Energy (in eV) of frontier molecular orbitals for the conformers of 1,4-Bis(1-methyl-2-benzimidazolyl)benzene.

	DFT/B3LYP/6-311++G(d,p)			
	Conformer1	Conformer2	Conformer3	Conformer4
HOMO−1	−6.3574	−6.3613	−6.3629	−6.3610
HOMO	−5.9819	−5.9523	−5.9931	−5.9740
LUMO	−1.8599	−1.8828	−1.8395	−1.8806
LUMO+1	−0.8232	−0.8223	−0.8555	−0.8340
ΔL–H	4.1220	4.0695	4.1536	4.0934

causes the torsion angle of N2—C7—C8—C9 is 1.21° larger than the torsion angle of N1—C7—C8—C10[i].

The imine (C=N) bond length is expected to be shorter than the amine (C—N) bond length. In the title molecule the imine C7=N1 and amine C7—N2 bond distances are 1.320(15) Å and 1.372(15) Å. The close proximity of the values with each others may be due to the electronic delocalization effect resulted from the super-conjugation system formed in the whole benzimidazole condensed ring. These bond lengths are in good agreement with values of 1-(Thiophen-2-yl-methyl)-2-(thiophen-2-yl)-1*H*-benzimidazole [1.315(3) and 1.387(3) Å] [31], 2-(4-Chlorophenyl)-1-methyl-1*H*-benzo[d]imidazole [1.330(3) and 1.380(3) Å] [9] and 1,4-Bis[(2-ethyl-1H-benzimidazol-1-yl)methyl]benzene [1317(5) and 1372(5) Å] [32].

The XRD results showed that there are no intermolecular hydrogen-bondings and intramolecular interactions in the molecular structure, but the molecular packing is stabilized by van der Waals forces. The crystal structure is further stabilized by five weak intermolecular interactions, one of them being a C—H···C_g(π-ring) contact and four of the rest being C—H···N contacts. The details of the intermolecular interactions in the molecule are listed in Table 4.

It might be worth mentioning that the largest difference between experimental and calculated geometrical parameters are about 0.0184 Å for bond lengths, 1.38° for angles and 7.42° for torsion angles and the root mean square deviation (RMSD) is found to be about 0.0072 Å for bond lengths, 0.56° for angles and 2.84° for torsion angles, indicating that B3LYP method correlates well with the XRD results for the geometric parameters. However, it was noted here that the experimental results belong to solid phase and the theoretical calculations belong to gaseous phase. In the solid state, the existence of the crystal field along with five weak intermolecular interactions has connected the molecules together, which result in the maximum differences of geometrical parameters (1-methylimidazole moiety of benzimidazole) between the calculated and experimental values.

To understand the influence of the structural features of the conformers of BMBB, energies of the frontier molecular orbitals were calculated at B3LYP/6-311++G(d,p) theory level. It is well known that both the highest occupied molecular orbital (HOMO) and lowest unoccupied molecular orbital (LUMO) are the main orbitals taking part in chemical reactions. The HOMO energy characterizes the ability of electron giving, LUMO energy characterizes the ability of electron accepting, and the gap between HOMO and LUMO characterizes the molecular chemical stability [33]. The distributions and energy levels of the HOMO–LUMO orbitals for each conformer was listed in Table 5 and was also depicted in Fig. 2. As seen from the figure, both the HOMO and LUMO are mainly delocalized among all atoms. However, the HOMO−1 and LUMO+1 orbitals are partially localized on different parts of the conformers. The HOMO−1orbitals are delocalized on the benzimidazole ring, while LUMO+1 orbitals are delocalized on the benzene ring. Both of the HOMOs and LUMOs are mostly π-antibonding type orbitals. The energy gap value between HOMO and LUMO is found around 4.1 eV for the four stable conformers. This low value makes the BMBB molecule more reactive.

Additionally, main atomic charges (i.e. the charges on non hydrogen atoms computed by natural population analysis) were also calculated at the same theory level and were listed in Table 6. According to atomic charge results, the common atoms in these conformers such as C2, C3, C4, C11, N1, and N2 possess richly negative charges, which are beneficial to the bioactivity [34].

Vibrational spectra

The XRD results indicated that the unit cell contains two molecules; each is at C_i symmetry. The free molecule has 126 normal vibrational modes and belongs to C_i point group,

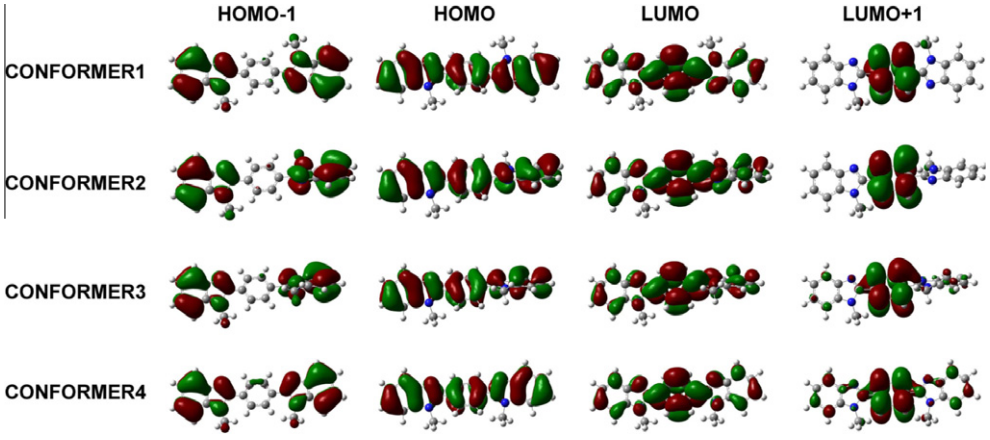

Fig. 2. HOMO−1, HOMO, LUMO and LUMO+1 molecular orbital surfaces for the conformers of 1,4-Bis(1-methyl-2-benzimidazolyl)benzene. The positive phase is red and the negative phase is green. (For interpretation of the references to color in this figure legend, the reader is referred to the web version of this article.)

Table 6
NBO charges (in e) for the conformers of 1,4-Bis(1-methyl-2-benzimidazolyl)benzene.

Nucleus	DFT/B3LYP/6-311++G(d,p)			
	Conformer1	Conformer2	Conformer3	Conformer4
C1/C1[i]	0.144	0.144	0.143	0.144
C2/C2[i]	−0.243	−0.243	−0.243	−0.244
C3/C3[i]	−0.202	−0.202	−0.202	−0.202
C4/C4[i]	−0.220	−0.220	−0.220	−0.220
C5/C5[i]	−0.191	−0.191	−0.190	−0.190
C6/C6[i]	0.114[a]	0.114	0.113	0.114
C7/C7[i]	0.410[a]	0.410[a]	0.410[a]	0.410[a]
C8/C8[i]	−0.086[a]	−0.087[a]	−0.086[a]	−0.087[a]
C9/C9[i]	−0.190[a]	−0.191[a]	−0.164[a]	−0.174[a]
C10/C10[i]	−0.147[a]	−0.147[a]	−0.174[a]	−0.164[a]
C11/C11[i]	−0.357	−0.356	−0.356	−0.356
N1/N1[i]	−0.492	−0.491	−0.490	−0.489[a]
N2/N2[i]	−0.419	−0.420[a]	−0.421[a]	−0.421[a]

[a] Average value.

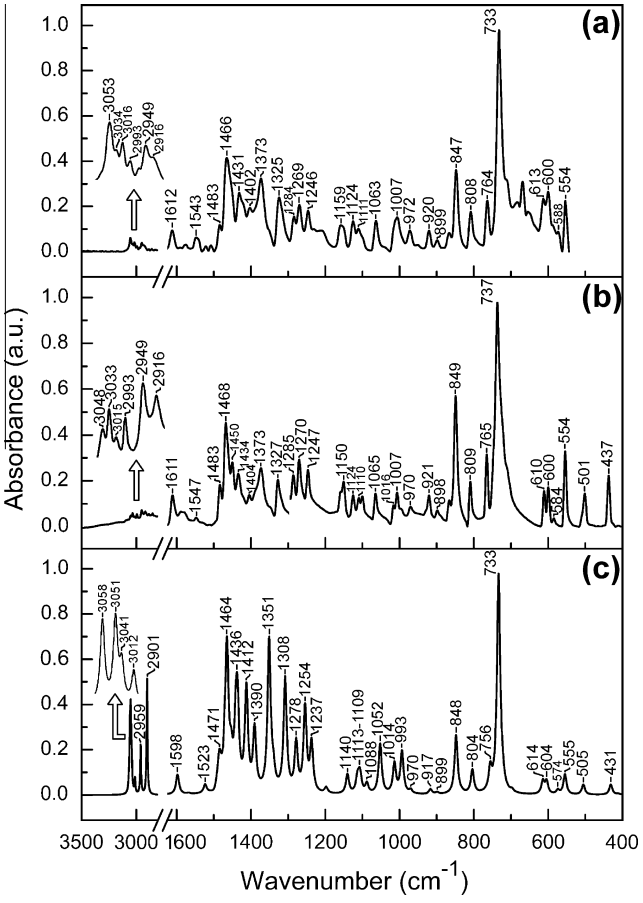

Fig. 3. The infrared spectra of 1,4-Bis(1-methyl-2-benzimidazolyl)benzene: (a) ATR–IR spectrum; (b) FT-IR spectrum in Nujol or 1,3-hexachlorobutadiene mulls; and (c) Conformer1, calculated.

$\Gamma_{vib}(C_i) = 53A_u + 53A_g$. Properties of the gerade (g) and ungerade (u) irreducible representations are symmetric and antisymmetric by application of the inversion operation. The fundamental transitions corresponding to the normal modes of A_g are Raman active only, whereas they are infrared active only for A_u [35].

Before offering an explanation for the vibrational assignments of BMBB molecule, FT-IR and dispersive Raman spectra along with the calculated spectra of Conformer1 were given in Figs. 3 and 4. The vibrational data of this comparison was also tabulated in Table 7; see also Tables S1 (Supporting Information) for the descriptions of all vibrational modes.

The absence of any bands in the region 3200–2700 cm^{-1} which is the characteristic N—H stretching mode for benzimidazole [36,37] indicates that N-methyl-o-phenylenediamine reacted to form benzimidazole ring. In addition, the absence of intermolecular hydrogen-bonding interactions in the molecule allows us to observe aromatic C—H stretching vibrations, easily. The C—H stretching vibrations of BMBB were assigned to three bands observed at 3053, 3034, 3016 cm^{-1} in the IR spectrum and 3065 cm^{-1} in the Raman spectrum. The calculated values of these bands are 3058, 3051, 3041 and 3058 cm^{-1} respectively with significant PED value ($\geqslant$94%). The asymmetric and symmetric aliphatic stretching vibrations of the methyl group are observed at 2993, 2949, 2916 cm^{-1} in the IR spectrum and 2952 cm^{-1} in the Raman spectrum. These bands were calculated at 3012 (PED 96%), 2959 (PED 97%), 2901 (PED 100%) and 2959 cm^{-1} (PED 97%). The characteristic C—H out of plane bending band of p-disubstituted benzene was observed at 847 (IR) and 842 cm^{-1} (Raman). The other infrared active very strong intense band at 733 cm^{-1} and the weak band at 920 cm^{-1} were assigned to C—H out of plane bending of benzimidazole rings. The calculated C—H out of plane bending mode values for p-disubstituted benzene ring at 848 cm^{-1} (PED 68%), 836 cm^{-1} (PED 99%) and for benzimidazole rings at 733 cm^{-1} (PED 66%) and 917 cm^{-1} (PED 66%) are in excellent agreement with experimental observation. The experimental values are well agreement with theoretical values [36,37].

The characteristic regions of the benzimidazole derivatives spectrum is 1650–1500 cm^{-1} which generally includes C=C stretching vibrations [38]. All substituted derivatives have bands in this region that vary in position and intensity with the nature and position of substituent. The IR active bands at 1612 and 1543 cm^{-1} were assigned to C=C stretching vibrations of the benzimidazole and the benzene rings respectively, which were calculated at 1598 cm^{-1} (PED 58%) and 1523 cm^{-1} (PED 32%). Their counterparts in Raman spectrum were at 1617 and 1563 cm^{-1} which were calculated at 1599 cm^{-1} (PED 49%) and 1544 cm^{-1} (PED 61%).

The identification of C=N and C—N vibrations are rather difficult since, the mixing of vibrations is possible in this region. However, with the help of the theoretical calculations, these vibrations are identified and assigned easily. The bands at 1466 and

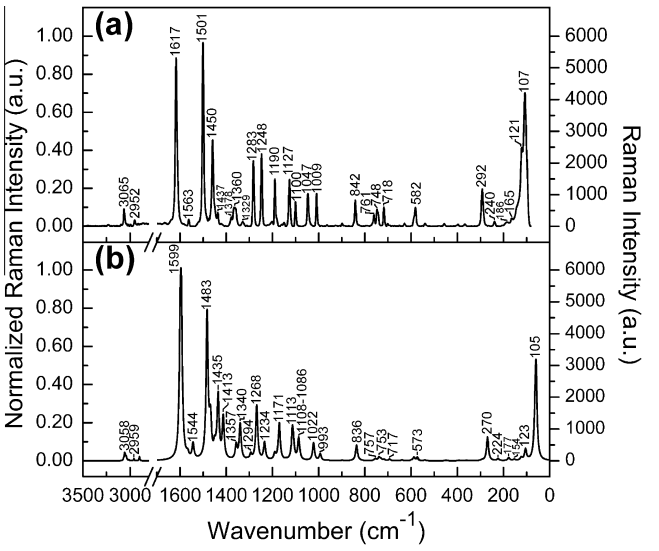

Fig. 4. The Raman spectra of 1,4-Bis(1-methyl-2-benzimidazolyl)benzene: (a) dispersive Raman spectrum; (b) Conformer1, calculated.

Table 7
The experimental vibrational assignments of 1,4-Bis(1-methyl-2-benzimidazolyl)benzene and comparison with the calculated data of Conformer1.

Mode	Experimental[a]				B3LYP/6-311++G(d,p)				
	Assignments	IR(solid)	IR(Nujol)	Raman(solid)	ν[c]	ν[d]	NI_{IR}[e]	I_{Raman}[e]	PED (potential energy distributions)[f] ⩾ 3
124,Ag	C—H stretch			3065 vw	3195	3058	0.00	0.05	$\nu R_{1,2}C3,4,5—H_{ar}$ (94)
123,Au	C—H stretch	3053 vw	3048 vw[b]		3195	3058	0.25	0.00	$\nu R_{1,2}C3,4,5—H_{ar}$ (94)
121,Au	C—H stretch	3034 vw sh	3033 vw[b]		3187	3051	0.25	0.00	$\nu R_{1,2}C2,3,5—H_{ar}$ (99)
117,Au	C—H stretch	3016 vw	3015 vw[b]		3176	3041	0.10	0.00	$\nu R_{1,2}C—H_{ar}$ (100)
113,Au	C—H_3 asymmetric stretch	2993 vw	2993 vw[b]		3146	3012	0.07	0.00	$\nu_{as}C—H_{methyl}$ (96)
112,Ag	C—H_3 asymmetric stretch			2952 vw	3091	2959	0.00	0.01	$\nu_{as}C—H_{methyl}$ (97)
111,Au	C—H_3 asymmetric stretch	2949 vw	2949 vw[b]		3091	2959	0.22	0.00	$\nu_{as}C—H_{methyl}$ (97)
109,Au	C—H_3 symmetric stretch	2916 vw sh	2916 vw[b]		3030	2901	0.51	0.00	$\nu_{s}C—H_{methyl}$ (100)
108,Ag	C=C stretch			1617 vs	1652	1599	0.00	0.72	$\nu R_{1,2}C=C_{ar}$ (49)
107,Au	C=C stretch	1612 w	1611 vw		1650	1598	0.09	0.00	$\nu R_{1,2}C=C_{ar}$ (58)
103,Ag	C=C stretch			1563 vw	1595	1544	0.00	0.10	$\nu RC=C_{ar}$ (61)+$\delta RC—H_{ar}$ (12)
102,Au	C=C stretch	1543 vw br	1547 vw		1572	1523	0.04	0.00	$\nu RC=C_{ar}$ (32)+$\nu_{as}C7—C8$ (14)+$\nu R_{1,2}C7=N1$ (10)
101,Ag	C=N stretch			1501 vs	1532	1483	0.00	1.00	$\nu R_{1,2}C7=N1$ (31)+$\nu_{s}C7—C8$ (14)+$\nu R_{1,2}C2—C3$ (7)
100,Au	C—H in-plane bend	1483 w	1483 w[b]		1520	1471	0.14	0.00	$\delta R_{1,2}C—H3,4$ (29)+$\nu R_{1,2}C2,4—C3,5$ (20)
98,Au	C=N stretch	1466 m	1468 m[b]		1508	1464	0.60	0.00	$\nu R_{1,2}C7=N1$ (26)+$\delta RC9—H_{ar}$ (22)+$\nu RC8—C10i$ (7)
93,Au	C—H_3 asymmetric deformation		1450 w[b]		1486	1436	0.34	0.00	$sciC—H_{methyl}$ (58)
92,Ag	C—H_3 asymmetric deformation			1450 m	1482	1435	0.00	0.43	$sciC—H_{methyl}$ (29)
91,Ag	C—H_3 symmetric deformation			1437 vw	1465	1413	0.00	0.29	$wC—H_{methyl}$ (66)
90,Au	C—H_3 symmetric deformation	1431 w	1434 w[b]		1463	1412	0.45	0.00	$wC—H_{methyl}$ (47)
89,Au	C—H in-plane bend	1402 w	1404 w[b]		1434	1390	0.27	0.00	$\delta RC—H_{ar}$ (30)+$\nu RC9—C10$ (25)
88,Ag	C—N strech/aromatic			1378 vw	1401	1357	0.00	0.10	$\nu R_{1,2}C7—N2$ (21)+$\nu_{s}R_{1,2}N2—C11$ (14)
87,Au	C—N strech/aromatic	1373 m	1373 w[b]		1395	1351	0.67	0.00	$\nu R_{1,2}C7—N2$ (18)+$\nu_{as}R_{1,2}N2—C11$ (15)+$\nu RC9—C10$ (8)+$\delta RC9—H9$ (6)
86,Ag	C=C stretch			1360 w br	1387	1340	0.00	0.25	$\nu R_{1,2}C=C_{ar}$ (28)+$\delta R_{1,2}C—H3$ (18)+$\nu R_{1,2}C1—N2$ (14)
83,Au	C—H in-plane bend	1325 w	1327 w[b]		1350	1308	0.50	0.00	$\delta R_{1,2}C—H2,4$ (15)+$\nu R_{1,2}C7=N1$ (11)+$\nu R_{1,2}C2—C3$ (10)+$\nu R_{1,2}C1—N2$ (10)
82,Ag	C—H in-plane bend			1329 vw br	1333	1294	0.00	0.04	$\delta RC—H_{ar}$ (68)
81,Au	C=C stretch/aromatic	1284 w	1285 w		1321	1278	0.22	0.00	$\nu_{as}RC—C—C_{trg}$ (24)+$\delta R_{1,2}C—H4,5$ (21)+$\nu R_{1,2}C6—N1$ (13)
80,Ag	C=C stretch/aromatic			1283 m	1308	1268	0.00	0.38	$\nu RC=C_{ar}$ (54)+$\nu R_{1,2}C7=N1$ (8)
79,Au	C—H in-plane bend	1269 w	1270 w		1300	1254	0.37	0.00	$\delta R_{1,2}C—H4,5$ (25)+$\nu R_{1,2}C6—N1$ (17)+$\nu R_{1,2}C4—C5$ (9)+$\nu R_{1,2}C7=N1$ (7)
78,Au	C—N strech/aromatic	1246 w	1247 w		1278	1237	0.22	0.00	$\nu R_{1,2}C6—N1$ (28)+$\nu R_{1,2}C7=N1$ (8)+$\nu R_{1,2}C1—C6$ (8)
77,Ag	C—N strech/aromatic			1248 m	1278	1234	0.00	0.12	$\nu R_{1,2}C6—N1$ (29)+$\nu R_{1,2}C7=N1$ (9)+$\nu R_{1,2}C1—C6$ (7)
74,Ag	C—H in-plane bend			1190 w	1209	1171	0.00	0.25	$\delta RC—H_{ar}$ (71)+$\nu RC9—C10$ (12)
72,Au	C—H in-plane bend	1159 w br	1150 w		1177	1140	0.08	0.00	$\delta R_{1,2}C—H2,3,4$ (78)+$\nu_{as}R_{1,2}C2—C3—C4$ (20)
71,Au	C—H_3 asymmetric deformation	1124 w	1124 w		1147	1113	0.06	0.00	$twC—H_{methyl}$ (72)
70,Ag	C—H_3 asymmetric deformation			1127 w	1146	1113	0.00	0.21	$twC—H_{methyl}$ (75)
69,Au	C—H in-plane bend	1111 w	1110 w		1143	1109	0.03	0.00	$\delta R_{1,2}C—H4,5$ (33)+$\nu R_{1,2}C2,4—C3,5$ (18)+$twC—H_{methyl}$ (16)
68,Ag	C—H in-plane bend			1100 w	1143	1108	0.00	0.10	$\delta R_{1,2}C—H4,5$ (33)+$\nu R_{1,2}C2,4—C3,5$ (22)+$twC—H_{methyl}$ (16)
64,Au	C—H_3 rock + C—N strech/ aromatic	1063 w	1065 w		1077	1052	0.22	0.00	$\rho C—H_{methyl}$ (19)+$\nu R_{1,2}C7—N2$ (19)+$\nu RC8—C10^{i}$ (11)+$\delta_{s}RC9—C8—C10^{i}$ (8)
63,Ag	Ring breath			1047 w	1054	1022	0.00	0.12	R breathing (37)+$\nu R_{1,2}C7—N2$ (18)
62,Au	C—C—C asymmetric in-plane bend		1016 w		1030	1014	0.13	0.00	$\delta_{as}RC—C—C_{trg}$ (67)+$\nu_{as}RC9—C8—C10^{i}$ (28)
61,Ag	C=C strech			1009 w	1028	993	0.00	0.05	$\nu_{s}R_{1,2}C2,3,4—C3,4,5(69)$
60,Au	C=C strech	1007 w	1007 w		1028	993	0.19	0.00	$\nu_{s}R_{1,2}C2,3,4—C3,4,5$ (69)
59,Au	C—H out-of-plane bend	972 vw	970 vw		994	970	0.02	0.00	$\gamma RC—H_{ar}$ (82)
55,Au	C—H out-of-plane bend	920 vw	921 vw		940	917	0.02	0.00	$\gamma R_{1,2}C—H_{ar}$ (66)
52,Au	C—N strech/aromatic	899 vw	898 w		911	899	0.01	0.00	$\nu R_{1,2}C—N_{ar}$ (33)+$\delta_{as}R_{1,2}C—C—C_{trg}$ (20)
51,Au	C—H out-of-plane bend	847 m	849 s		868	848	0.26	0.00	$\gamma RC—C—H_{ar}$ (68)
50,Ag	C—H out-of-plane bend			842 w	857	836	0.00	0.11	$\gamma RC—C—H_{ar}$ (99)
46,Au	C=C strech	808 w	809 w		827	804	0.10	0.00	$\nu R_{1,2}C=C_{ar}$ (34)+$\nu R_{1,2}C6—N1$ (7)
45,Ag	Ring asymmetric deformation			761 vw	776	757	0.00	0.01	$d_{as}R_{1,2}$ (29)
44,Au	Ring asymmetric deformation	764 w	765 m		775	756	0.10	0.00	$d_{as}R_{1,2}$ (49)
43,Ag	C=C out-of-plane bend			748 vw	771	753	0.00	0.02	$\gamma RC=C_{ar}$(36)
41,Au	C—H out-of-plane bend	733 vs	737 vs		752	733	1.00	0.00	$\gamma R_{1,2}C—H_{ar}$ (66)
38,Ag	C—C—C symmetric in-plane bend			718 w	725	717	0.00	0.01	$\delta_{s}RC—C—C_{trg}$ (13)+$\delta_{as}C7—C8—C9$ (9)+$\nu RC8—C10^{i}$ (8)
34,Au	C—C—C symmetric in-plane bend	613 w	610 w		620	614	0.06	0.00	$\delta_{s}R_{1,2}C—C—C_{trg}$ (18)+$\delta_{s}R_{1,2}C2—C1—N2$ (8)+$\nu_{as}C7—C8$ (7)
33,Au	C—C—C symmetric in-plane bend	600 w	600 w		608	604	0.06	0.00	$\delta_{s}R_{1,2}C—C—C_{trg}$ (18)+$\delta_{s}C8—C7=N_{ar}$ (14)

30,Au	C=C out-of-plane bend	588 w	584 vw		588	574	0.02	0.00	$\gamma R_{1,2}C{=}C_{ar}$ (63)
29,Ag	C=C out-of-plane bend			582 w	587	573	0.00	0.02	$\gamma R_{1,2}C{=}C_{ar}$ (62)
28,Au	Ring breath	554 w	554 m		562	555	0.09	0.00	$R_{1,2}$ breathing (34)+$\nu_{as}R_{1,2}N2{-}C11$ (16)
26,Au	Ring torsion		501 w		515	505	0.04	0.00	$\tau RC{=}C_{ar}$ (38)
24,Au	Ring torsion		437 w		442	431	0.05	0.00	$\tau R_{1,2}C{=}C_{ar}$ (34)
15,Ag	Ring torsion			292 w	275	270	0.00	0.16	$\tau R_{1,2}$ (23)
13,Ag	Ring torsion			240 vw	228	224	0.00	0.01	$\tau R_{1,2}$ (32)+$\gamma_s C7{-}C8{-}C9$ (6)
12,Ag	$C{-}H_3$ torsion			186 vw br	182	177	0.00	0.02	$\tau C{-}H_{methyl}$ (28)+$\nu_s C7{-}C8$ (13)
10,Ag	Rings symmetric stretch + $C{-}H_3$ torsion			165 vw	157	154	0.00	0.01	$\nu_s C7{-}C8$ (19)+$\tau C{-}H_{methyl}$ (19)+$\delta_s RC8{-}C9{-}C10_{trg}$ (9)
8,Ag	Ring-CH_3 twist			121 m	126	123	0.00	0.02	$twR_{1,2}{-}CH_{methyl}$ (76)
6,Ag	Rings wag			107 s	106	105	0.00	0.07	$\gamma_s C8{-}C7{-}N_{ar}$ (40)+$\tau_s C7{-}C8$ (12)

[a] s: Strong, m: medium, w: weak, v: very, sh: shoulder and br: broad.
[b] The infrared active vibrational wavenumbers are obtained in hexachloro-1,3-butadiene.
[c] Unscaled vibrational wavenumbers.
[d] Wavenumbers are scaled by SQM FF methodology (See the text).
[e] NI: Intensities are normalized to 1, *I*: Intensity, IR: infrared and the relative intensities of the simulated spectra were obtained after using the pure Lorentzian band shape a bandwidth 10 cm^{-1}.
[f] R: benzene ring, R_1 and R_2: benzimidazole rings, ar: aromatic, ν: bond stretching, δ: in-plane angle bending, γ: out-of-plane angle bending, sci: scissoring, w: wagging, tw: twisting, ρ: rocking, d: deformation, τ: torsion, trg: trigonal, as: asymmetric and s: symmetric.

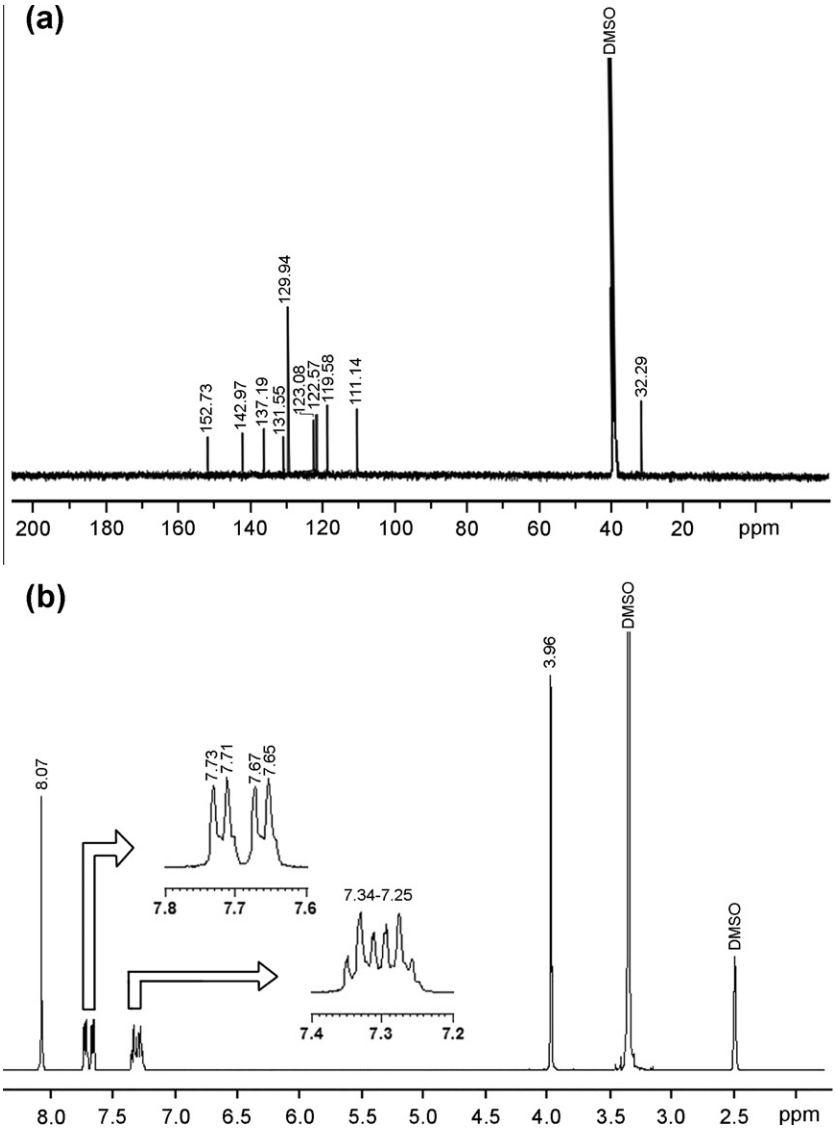

Fig. 5. The NMR spectra of 1,4-Bis(1-methyl-2-benzimidazolyl)benzene in DMSO-d_6: (a) ^{13}C; (b) ^{1}H.

Table 8
The experimental ^{13}C and ^{1}H NMR chemical shifts (ppm) together within the calculated data for the stable conformers of BMBB in DMSO-d_6.

Nucleus	Experimental	B3LYP/6-311++G(d,p)[a]			
		Conformer1	Conformer2	Conformer3	Conformer4
C7	152.73	153.85	154.23	154.69	153.29
C6	142.97	143.84	144.03	143.99	143.99
C1	137.19	138.27	138.20	138.11	138.25
C8	131.55	132.36	132.25	132.58	132.67
C9,10i	129.94	129.83	129.79	130.00	129.97
C3	123.08	123.77	123.54	124.01	123.85
C4	122.57	122.47	122.47	122.74	122.60
C5	119.58	119.79	119.78	119.87	119.87
C2	111.14	109.50	109.31	109.21	109.44
C11	32.29	31.00	31.15	31.19	31.21
H—C9,10i	8.07 s	8.22	8.25	8.17	8.25
H—C5	7.72 d	7.99	8.00	8.00	8.00
H—C2	7.66 d	7.74	7.73	7.70	7.71
H—C4,C3	7.34–7.25 m	7.71–7.61	7.68–7.59	7.72–7.67	7.64–7.63
H—C11	3.96 s	3.89	3.95	3.88	3.97

[a] σ Transform into δ using equations given in Ref. [10]; $\delta^{13}C = 175.7–0.963\ \sigma^{13}C$ and $\delta^{1}H = 31.0–0.970\ \sigma^{1}H$.

1373 cm^{-1} (IR) and at 1501 and 1378 cm^{-1} (Raman) were assigned to C═N and C—N vibrations. These values support the reported results [8,9,38–42].

The low wavenumber region generally gives more qualified information about the conformational behaviors of the compounds [7,10]. Computational vibrational wavenumbers in this region (below 600 cm^{-1}) are sensitive than the high wavenumber region. As clearly seen from Table 7, the computed wavenumbers are great agreement with the experimental ones. This agreement tends us to make more reliable vibrational assignment of title compound. The skeletal vibrations, such as C═C═C out-of-plane bending, ring breathing, ring or CH_3 torsion vibrations are undoubtedly assigned.

It might be worth mentioning that RMS error and correlation of the wavenumbers between experimental and theoretical wavenumbers were found to be 7.93 cm^{-1} and 0.9998.

NMR spectra

The ^{13}C and ^{1}H NMR spectra using TMS as an internal standard and DMSO-d_6 as solvent are shown in Fig. 5. The experimental ^{13}C and ^{1}H NMR chemical shifts (ppm) together within the calculated data for the stable conformers of the BMBB are given in Table 8. As can be clearly seen from the table, calculated data for all stable conformers are nearly in accordance with the experimental values. This shows that, BMBB molecule can be existed in each one of all conformers in liquid phase.

The singlet signal at the lowest field (8.07 ppm) accounting for four protons was easily assigned to equivalent protons of the 1,4-disubstituted benzene ring (H—C9,10,9i,10i). H—C5 and H—C2 protons appeared as two different doublet signals at 7.72 and 7.66 ppm, respectively. H—C4 and H—C3 protons appeared together as multiplet at the region 7.34–7.25 ppm. The protons of the methyl group (H—C11) at the benzimidazole ring appeared as singlet signal at 3.96 ppm. There are two very simple peaks in the ^{13}C NMR spectrum which could be identified clearly. The first peak at 32.28 ppm is certainly belongs to methyl group which is the single aliphatic carbon atom in the structure. The second peak at 152.73 ppm is assigned to C7 carbon in C═N form which supports the formation of the benzimidazole ring. The tallest peak at 129.94 ppm must be due to the four carbons of the benzene ring (C9, C10, C9i, C10i) which are both in the same environment. As shown in Fig. 5, all the other carbons in the benzimidazole ring appear separately at the expected regions. Consequently, the experimental ^{1}H and ^{13}C spectra data also support the structure of the title compound and in accordance with reported values [43,44].

Conclusion

The conformational analysis results indicated that 1,4-Bis(1-methyl-2-benzimidazolyl)benzene compound has four stable conformers at room temperature. The relative energies and population analysis were showed that Conformer1 is the most stable form. The molecular structure of 1,4-Bis(1-methyl-2-benzimidazolyl)benzene was characterized by single-crystal X-ray diffraction, FT-IR, dispersive Raman, ^{1}H-NMR and ^{13}C-NMR spectroscopies. The molecular properties of the Conformer1 such as, geometrical parameters, vibrational and NMR data were also determined at DFT-B3LYP/6-311++G(d,p) theory level and were compared with experimental spectroscopic findings.

The general agreement with theoretical calculations and single-crystal structure was in a good range, even as a few differences observed in the geometrical parameters. These differences were completely observed in 1-methylimidazole moiety of BMBB which was affected by weak intermolecular interactions in the crystal field. The frontier molecular orbitals and natural bond orbitals analyses on all stable conformers showed that 1,4-Bis(1-methyl-2-benzimidazolyl)benzene is a potential candidate for bioactivity studies.

The sufficient consistency between the experimental and calculated wavenumbers of 1,4-Bis(1-methyl-2-benzimidazolyl)benzene molecule allowed us to safely assign the complete vibrational spectrum. Any differences observed between the experimental and the calculated wavenumbers was thought to be the fact that, the calculations have been performed for single molecule in the gaseous state contrary to the experimental values which recorded in the presence of intermolecular interactions or solid-state effects.

The calculated NMR shifts of four stable conformers were nearly consistence with the experimental values. This suggests that, the molecule could be existed in each one of all conformers due to the intermolecular interactions in liquid phase.

Acknowledgements

This study was supported financially by Bilecik Şeyh Edebali University (Project No: 2011-02-BİL.04-03). We would like to thank also to Dr. Hakan Dal for XRD measurement.

Appendix A. Supplementary material

Supplementary data associated with this article can be found, in the online version, at http://dx.doi.org/10.1016/j.saa.2012.10.055.

References

[1] J.B. Foresman, A. Frisch, Exploring Chemistry with Electronic Structure Methods, second ed., Gaussian, Inc., Pittsburgh, 1996.
[2] W. Koch, M.C. Holthausen, A Chemist's Guide to Density Functional Theory, Wiley-VCH, 2000.
[3] A.D. Becke, J. Chem. Phys. 98 (1993) 5648–5652.
[4] H. Arslan, Ö Algül, Y. Dündar, Vib. Spectrosc. 44 (2007) 248–255.
[5] R.K. Srivastava, V. Narayan, O. Prasad, L. Sinha, J. Chem. Pharm. Res. 4 (2012) 3287–3296.
[6] N. Sundaraganesan, S. Ilakiamani, B. Dominic Joshua, Spectrochim. Acta Part A 67 (2007) 287–297.
[7] A. Ünal, M. Şenyel, Ş. Şentürk, Vib. Spectrosc. 50 (2009) 277–284.
[8] N. Özdemir, B. Eren, M. Dinçer, Y. Bekdemir, Mol. Phys. 108 (2010) 13–24.
[9] N. Özdemir, B. Eren, M. Dinçer, Y. Bekdemir, Int. J. Quantum Chem. 111 (2011) 3112–3124.
[10] H. Alyar, S. Alyar, A. Ünal, N. Özbek, E. Şahin, N. Karacan, J. Mol. Struct. 1028 (2012) 116–125.
[11] H. Alyar, A. Ünal, N. Özbek, S. Alyar, N. Karacan, Spectrochim. Acta Part A 91 (2012) 39–47.

[12] N.M. Aghatabay, A. Neshat, T. Karabiyik, M. Somer, D. Haciu, B. Dülger, Eur. J. Med. Chem. 42 (2007) 205–213.
[13] N.M. Aghatabay, B. Dülger, F. Gucin, Eur. J. Med. Chem. 38 (2003) 875–881.
[14] H. Küçükbay, Ü. Yılmaz, N. Şireci, A.N. Önganer, Turk. J. Chem. 35 (2011) 561–571.
[15] M. Del Poeta, W.A. Schell, C.C. Dykstra, S. Jones, R.R. Tidwell, A. Czarny, M. Bajić, Ma. Bajić, A. Kumar, D. Boykin, J.R. Perfect, Antimicrob. Agents Chemother. 42 (1998) 2495–2502.
[16] M. Singh, V. Tandon, Eur. J. Med. Chem. 46 (2011) 659–669.
[17] I. Stolić, K. Mišković, A. Magdaleno, A.M. Silber, I. Piantanida, M. Bajić, L. Glavaš-Obrovac, Bioorg. Med. Chem. 17 (2009) 2544–2554.
[18] Q. Sun, B. Gatto, C. Yu, A. Liu, L.F. Liu, E.J. LaVoie, Bioorg. Med. Chem. Lett. 4 (1994) 2871–2876.
[19] Y. Fu, W. Li, A. Manthriam, J. Membrane Sci. 310 (2008) 262–267.
[20] K. Hung-Lin, Y.-H. Lee, S.-T. Huang, C. Su, T.C.-K. Yang, Sol. Energy Mater Sol. C 95 (2011) 158–162.
[21] H.F. Ridley, R.G.W. Spickett, G.M. Timmis, J. Heterocyclic Chem. 2 (1965) 453–456.
[22] Mopac-PM5 implemented in CAChe WorkSystem Pro. ver. 7.5.0 for Windows, Fujitsu Co. Ltd., Japan, 2006.
[23] C. Lee, W. Yang, R.G. Parr, Phys. Rev. B 37 (1988) 785–789.
[24] M.J. Frisch, et al., Gaussian 03 Revision D.01, Gaussian Inc., Wallingford, CT, 2004.
[25] SQM version 1.0, Scaled Quantum Mechanical, Green Acres Road, Fayetteville, Arkansas 72703, 2013.
[26] J. Baker, A.A. Jarzecki, P. Pulay, J. Phys. Chem. A 102 (1998) 1412–1424.
[27] M. Cossi, V. Barone, B. Mennucci, J. Tomasi, Chem. Phys. Lett. 286 (1998) 253–260.
[28] J. Tomasi, B. Mennucci, E. Cances, J. Mol. Struct.-Theochem. 464 (1999) 211–226.
[29] K. Wolinski, J.F. Hinton, P. Pulay, J. Am. Chem. Soc. 112 (1990) 8251–8260.
[30] J.R. Cheeseman, G.W. Trucks, T.A. Keith, M.J. Frisch, J. Chem. Phys. 104 (1996) 5497–5509.
[31] M. Sekerci, Y. Atalay, F. Yakuphanoglu, D. Avcı, A. Başoğlu, Spectrochim. Acta Part A 67 (2007) 503–508.
[32] Q. Wang, Z. Zhao, H. Lou, M. Wang, Acta Cryst. E67 (2011) o1899.
[33] I. Fleming, Frontier Orbitals and Organic Chemical Reactions, Wiley, London, 1976.
[34] P. Chavatte, S. Yous, C. Marot, N. Baurin, D. Leiseur, J. Med. Chem. 44 (2001) 3223–3230.
[35] F.A. Cotton, Chemical Applications of Group Theory, John Wiley & Sons, Inc., New York, 1965.
[36] G. Varsanyi, Assignments for Vibrational Spectra of Seven Hundred Benzene Derivatives, vol. 1, Adam Hilger, London, 1974.
[37] D. Lin-vien, N.B. Colthup, W.G. Fateley, J.G. Grasselli, The Hand Book of Infrared and Raman Characteristic Frequencies of Organic Molecules, Academic Press, New York, 1990.
[38] P.N. Preston, The Chemistry of Heterocyclic Compounds: Benzimidazoles and Cogeneric Tricyclic Compounds, John Wiley & Sons. Inc., New York, 2009.
[39] C. James, C. Ravikumar, V.S. Jayakumar, I. Hubert Joe, J. Raman Spectrosc. 40 (2009) 537–545.
[40] T.D. Klots, P. Devlin, W.B. Collier, Spectrochim. Acta Part A 53 (1997) 2445–2456.
[41] R. Infante-Castillo, L.A. Rivera-Montalvo, S.P. Hernandez-Rivera, J. Mol. Struct. 877 (2008) 10–19.
[42] N. Sundaraganesan, S. Ilakiamani, P. Subramani, B. Dominic Joshua, Spectrochim. Acta Part A 67 (2007) 628–635.
[43] V. Sridharan, S. Saravanan, S. Muthusubramanian, S. Sivasubramanian, Magn. Reson. Chem. 43 (2005) 551–556.
[44] C.K. Lee, I.-S.H. Lee, Bull. Korean Chem. Soc. 29 (11) (2008) 2205–2208.